

Electrical characterization of 5.4 MeV alpha-particle irradiated 4H-SiC with low doping density

A. T. Paradzah, F.D. Auret, M.J. Legodi, E. Omotoso, M. Diale
Department of Physics, University of Pretoria, Pretoria 0002, South Africa

Abstract

Nickel Schottky diodes were fabricated on 4H-SiC. The diodes had excellent current rectification with about ten orders of magnitude between -50V and +2V. The ideality factor was obtained as 1.05 which signifies the dominance of the thermionic emission process in charge transport across the barrier. Deep level transient spectroscopy revealed the presence of four deep level defects in the 30 – 350 K temperature range. The diodes were then irradiated with 5.4 MeV alpha particles up to fluence of $2.6 \times 10^{10} \text{ cm}^{-2}$. Current - voltage and Capacitance - voltage measurements revealed degraded diode characteristics after irradiation. DLTS revealed the presence of three more energy levels with activation enthalpies of 0.42 eV, 0.62 eV and 0.76 eV below the conduction band. These levels were however only realized after annealing the irradiated sample at 200 °C and they annealed out at 400 °C. The defect depth concentration was determined for some of the observed defects.

Keywords: n-type 4H-SiC; Schottky diode; Deep Level Transient Spectroscopy (DLTS); Alpha particle irradiation; Defects

1. Introduction

Silicon Carbide (SiC) has excellent electronic and physical properties which include high electron drift velocity, high breakdown voltage, radiation hardness and high thermal conductivity [1]. These properties make SiC a suitable candidate for the fabrication of devices that can operate in harsh environments (exposed to radiation and/or at elevated temperatures).

Characteristics of electronic devices can be severely degraded by the presence of electrically active defects. The identification and control of as-grown and radiation induced defects is therefore important as the elimination or control of defect levels associated with these defects is required for effective device technology to progress [2]. While semiconductor materials have in-grown electronic defects, energetic particles such as electrons, protons, alpha particles, pions, neutrons and γ -ray photons can also cause bulk and/or surface damage in materials [3]. This damage leads to the formation of point defects and clusters resulting in the degradation of diode quality as they may lead to increased leakage current and decreased effective doping density [2].

It is therefore important to study and understand defects induced by radiation damage if a semiconductor is to be successfully used for fabrication of devices that can operate in harsh environments. Electron, proton and alpha particle irradiation has been performed on SiC to study the formation of defects and understand the hardness of the material. It has been observed from these studies that different types of irradiation induce the same types of defects in SiC but in different concentrations [4]. Alpha particle irradiation is however expected to cause more damage due to a superior mass compared to other forms of irradiation.

In this study, nickel Schottky contacts were fabricated on n-type 4H-SiC with a doping density of $3.7 \times 10^{14} \text{ cm}^{-3}$. Deep level transient spectroscopy was performed to study the defects in the as-grown material and also to assess how alpha irradiation modifies these defects. Current-Voltage (*I-V*) and Capacitance-Voltage (*C-V*) measurements were utilized to evaluate the effect of alpha irradiation on the quality of the diodes. Annealing studies were done to determine the thermal dynamics of both the as-grown and the radiation induced defects.

2. Experimental

4H-SiC with a low doping density of $\sim 4 \times 10^{14} \text{ cm}^{-3}$ was used in this study. Sample degreasing was done by boiling in trichloroethylene (TCE), acetone and methanol for 5-minutes in each solution. This was followed by rinsing in de-ionised water before a 30-second dip in hydrofluoric acid (HF) to remove the native oxide layer. This was followed by rinsing in de-ionised water and a blow-dry using N_2 gas. A 300 nm thick nickel ohmic contact was resistively deposited onto the highly doped ($1 \times 10^{18} \text{ cm}^{-3}$) back side and annealed in flowing argon for 20 minutes at 950 °C. Cleaning was repeated as before except that, instead of boiling, 3 minute rinsing in each of the three solvents were performed in an ultrasonic bath. Nickel Schottky contacts with a diameter of

0.6 mm and thicknesses of 100 nm were then resistively deposited onto the $3.7 \times 10^{14} \text{ cm}^{-3}$ doped side. Deep level transient spectroscopy (DLTS) measurements were carried out using a National Instruments Digital Acquisition (DAQ) based Laplace-DLTS system. Irradiation was done using a 5.4 MeV radioactive alpha source (Am-241) of dose rate $7.1 \times 10^6 \text{ cm}^{-2} \text{ s}^{-1}$ to fluences of up to $2.6 \times 10^{10} \text{ cm}^{-2}$. The diodes were annealed after irradiation in steps of 100 °C in flowing argon gas up to 600 °C. TRIM simulation projected the alpha particles to peak at a depth of 24.8 μm below the nickel ohmic. Maximum vacancy concentration was also projected at a depth of 24.8 μm as 0.014 per Angstrom – Ion, translating to $\sim 3.64 \times 10^{18}$ vacancies.

3. Results and Discussion

3.1 Current–voltage results

Forward I - V characteristics of the nickel Schottky contact before and after alpha irradiation to fluence of $2.6 \times 10^{10} \text{ cm}^{-2}$ (this fluence corresponds to 60 minutes of irradiation) are shown in Figure 1. A linear current–voltage relationship was obtained before irradiation and the fitting was done using a thermionic emission model given by the relation [5, 6]:

$$I_{S-M} = I_s [\exp(qV/nk_B T) - 1] \quad (1)$$

where I_{S-M} is the current flowing from the semiconductor into the metal, I_s is known as the saturation current, q is the electronic charge, V is the applied voltage, n is the ideality factor, k_B is the Boltzmann constant and T is the temperature at which the measurements were taken. The saturation current is given by the equation [5, 6]:

$$I = AA^*T^2 \exp(-q\Phi_{b0}/nk_B T) \quad (2)$$

A is the effective Schottky diode area, A^* is the Richardson constant and Φ_{b0} is the zero bias Schottky barrier height.

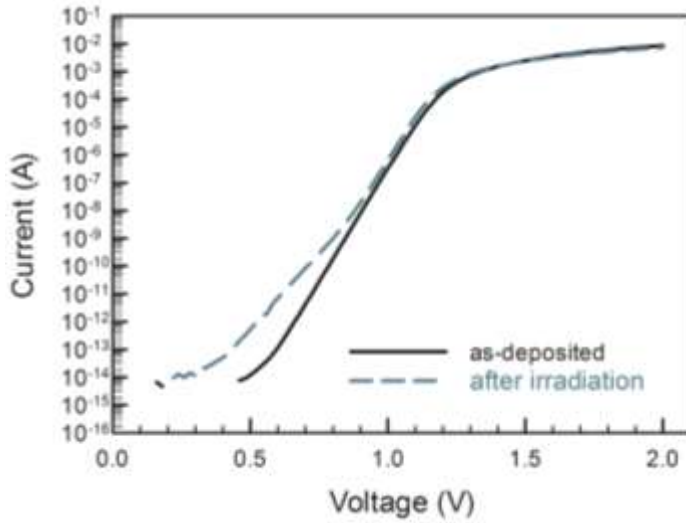


Figure 1 Forward current–voltage curves obtained before and after 5.4 MeV alpha particle irradiation to fluence of $2.6 \times 10^{10} \text{ cm}^{-2}$

The ideality factor is obtained from the gradient of the linear region of the I - V curves according to Eqn. (1). Before irradiation, the ideality factor was obtained as 1.05, a close to unity value which shows that the thermionic emission model describes current flow across the metal–semiconductor interface sufficiently. After irradiation to fluence of $2.6 \times 10^{10} \text{ cm}^{-2}$, the ideality factor increased to 1.35. The large ideality factor value obtained after irradiation implies that there are other current transport mechanisms in addition to the thermionic emission mechanism. The most probable additional current transport mechanism is generation–recombination current resulting from atomic displacements induced by alpha particle irradiation. This is also observed on the I - V curve obtained after irradiation, Figure 1, which is non-linear especially at low voltages where the effect of thermionic emission is minimal. The Schottky barrier height was obtained from I - V measurements following Eqn. (2). The Schottky barrier height was obtained as 1.21 eV before irradiation and an increase to 1.28 eV was observed after a total alpha-particle fluence of $2.6 \times 10^{10} \text{ cm}^{-2}$. The increase in the SBH is very small and this allows for the continued normal operation of the Schottky diodes.

The reverse leakage current was measured to voltages of -50 V. Reverse leakage current curves obtained before and after a total irradiation fluence of $2.6 \times 10^{10} \text{ cm}^{-2}$ are presented in Figure 2. Low leakage current values are observed showing good rectification quality of the SiC Schottky diodes. An increase in the leakage current is observed with increasing reverse bias. This is attributed to Schottky barrier lowering, a phenomena where the SBH is lowered as the electric field resulting from external biasing increases [7].

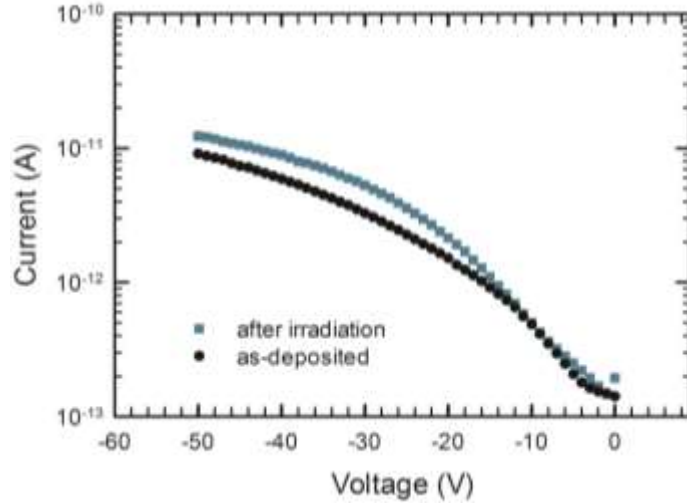


Figure 2 Reverse leakage current curves measured up to -50 V before and after alpha particle irradiation to fluence of $2.6 \times 10^{10} \text{ cm}^{-2}$

The reverse current obtained at -50 V increased from $9.0 \times 10^{-12} \text{ A}$ to $1.2 \times 10^{-11} \text{ A}$ after irradiation. The increase in the leakage current show the effect of irradiation where defects induced by irradiation are suggested to be responsible for the increase. However the diode rectification was retained after irradiation and this shows that SiC is a radiation hard semiconductor. The current measured at applied voltages of -50 V and +2 V changes by approximately ten orders of magnitude even after irradiation which shows good rectification of SiC.

3.2 Capacitance–voltage results

The effects of alpha–particle irradiation on the free carrier concentration and the SBH were evaluated using C-V measurements. The free carrier concentration N_D and the SBH Φ_{Bn} were respectively determined from the slope and the intercept of the graph of $1/C^2$ vs. V , Figure 3. N_D was obtained according to the relation [7]:

$$\frac{d(1/C^2)}{dV} = \frac{2}{A^2 \epsilon_0 \epsilon_s q N_D} \quad (3)$$

where C is the depletion width capacitance and ϵ_s is the semiconductor permittivity, and ϵ_0 is the permittivity of free space. The SBH was obtained from [7]

$$\Phi_{Bn} = V_{bi} + V_n + \frac{k_B T}{q} - \Delta\Phi \quad (4)$$

where $\Delta\Phi$ is the Schottky barrier lowering due to the image force effect, V_n is the depth of the Fermi level below the conduction band and is obtained from the relation:

$$V_n = \frac{k_B T}{q} \ln\left(\frac{N_c}{N_D}\right) \quad (5)$$

V_{bi} is the built in potential which is obtained as the voltage intercept of the linear C–V relationship, Figure 3 and N_c is the effective density of states in the conduction band.

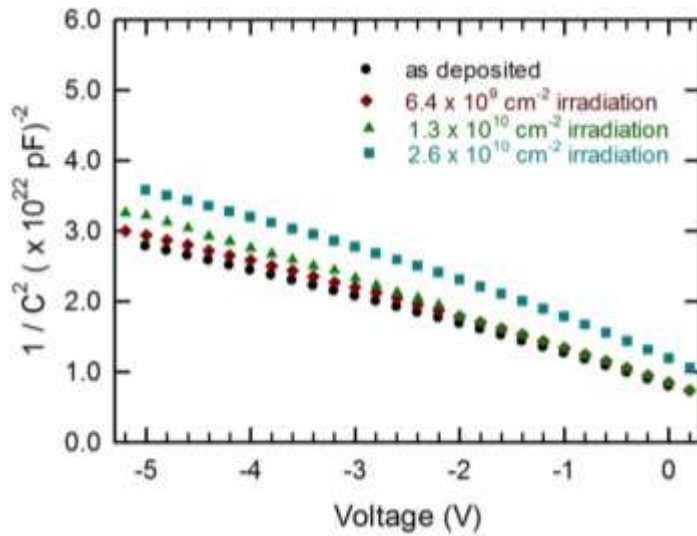


Figure 3 $1/C^2$ graphs obtained before and after alpha particle irradiation at indicated fluences to $2.6 \times 10^{10} \text{ cm}^{-2}$

The SBH was obtained as 1.86 eV before irradiation and it increased to 2.02 eV after irradiation to fluence of $2.6 \times 10^{10} \text{ cm}^{-2}$. The increase in the SBH can be seen from Figure 3 where the voltage intercept of the $1/C^2$ vs. V curve increases after irradiation. There were no major changes in the curves at intermediate irradiation fluences. The SBH obtained through capacitance–voltage measurements is larger than that obtained from current–voltage measurements. This is due to the inhomogeneity of the metal–semiconductor interface where electrons cross the junction via “small barrier regions” hence the smaller I – V measured SBH [8].

The free carrier concentration decreased from $4.9 \times 10^{14} \text{ cm}^{-3}$ before irradiation to $2.9 \times 10^{14} \text{ cm}^{-3}$ after irradiation to fluence of $2.6 \times 10^{10} \text{ cm}^{-2}$. Non-linear curves of $1/C^2$ against voltage, shows that the free carrier concentration is not constant below the metal–semiconductor junction. This is also shown by the depth profiles, Figure 4. The decrease in the free carrier concentration is an indication that defects were introduced by irradiation and the defects are of acceptor-like nature hence they trap the free carriers leading to the observed reduction. Some recovery in the free carrier concentration was observed after annealing the irradiated diodes at 200°C and annealing to 600°C did not lead to further recovery.

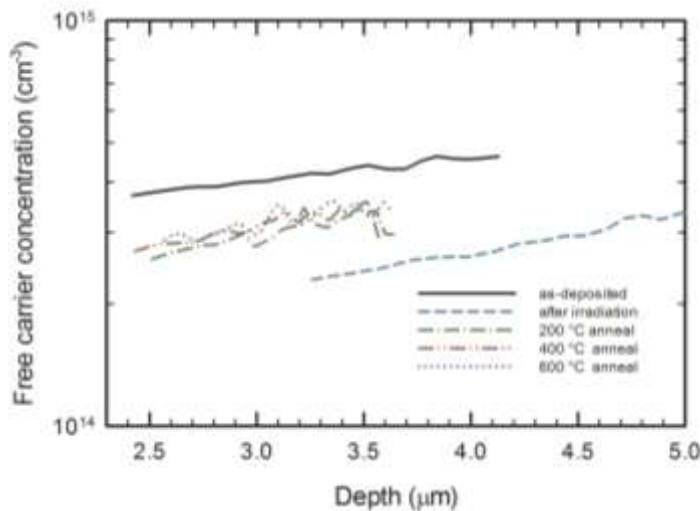


Figure 4 Free carrier concentration depth profiles obtained before irradiation, after alpha particle irradiation to fluence of $2.6 \times 10^{10} \text{ cm}^{-2}$ and at subsequent annealing temperatures

The reduction in the free carrier concentration with irradiation can be quantified by the free carrier removal rate. The free carrier removal rate is obtained from the slope of the graph of $\Delta(N_D - N_A)/\Phi$, Φ being the fluence and $\Delta(N_D - N_A)$ is the change in the free carrier concentration [9]. The free carrier removal rate was obtained after irradiating the diodes at three different fluences up to $2.6 \times 10^{10} \text{ cm}^{-2}$ as 15101 cm^{-1} . This is a large value and is

a result of the high energy (5.4 MeV) of the irradiating alpha particles. Alpha particles are also heavy particles compared to most particles used in irradiation studies hence more damage is realised leading to this large value.

The Schottky barrier parameters obtained before irradiation and after $2.6 \times 10^{10} \text{ cm}^{-2}$ alpha-particle irradiation are summarised in Table 1.

Table 1 Diode characteristics before and after 5.4 MeV alpha irradiation to fluence of $2.6 \times 10^{10} \text{ cm}^{-2}$.

	Ideality factor	$\Phi_{IV}(\text{eV})$	$\Phi_{CV}(\text{eV})$	Leakage current (A) at -50 V bias	Free carrier density (cm^{-3})
Before irradiation	1.05	1.21	1.86	9.0×10^{-12}	4.9×10^{14}
After irradiation	1.35	1.28	2.09	1.2×10^{-11}	2.9×10^{14}

3.3 DLTS results

The DLTS spectra obtained from the as-deposited material, Figure 5 shows the presence of four energy levels which have been labelled $E_{0.10}$, $E_{0.12}$, $E_{0.18}$ and $E_{0.69}$. These have activation energies of $E_c - 0.10 \text{ eV}$, $E_c - 0.12 \text{ eV}$, $E_c - 0.18 \text{ eV}$ and $E_c - 0.69 \text{ eV}$ respectively. The capture cross sections of the levels and respective attributions are presented in Table 2.

The defect $E_{0.10}$ has been attributed to nitrogen dopants occupying cubic sites [10, 11]. When occupying a hexagonal site in 4H-SiC, this defect level is expected to have an activation energy of $\sim 0.050 \text{ eV}$ [12, 13]. This level is the nitrogen donor responsible for the n -type doping in SiC.

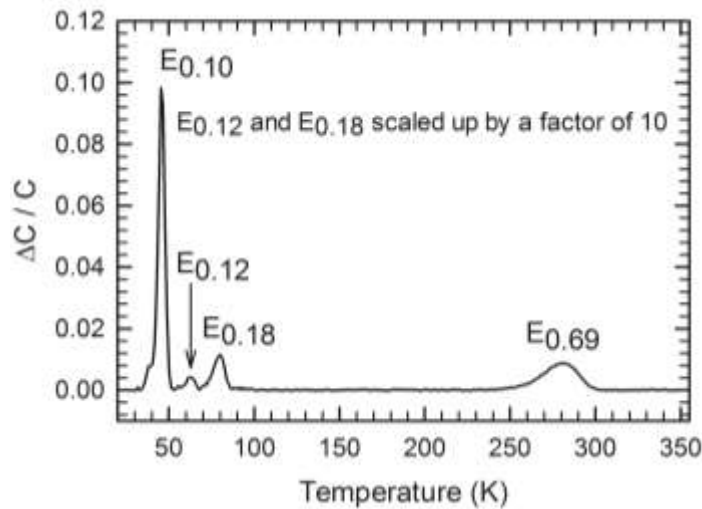


Figure 5 DLTS spectra for the as deposited sample. Spectra obtained at constant reverse bias of -5V, filling pulse of -1 V and rate window of 2.5 s^{-1}

The $E_{0.12}$ and $E_{0.18}$ levels are related to transitional metal titanium [11, 14]. To within experimental error, Ahtziger *et al.* [14] observed and attributed the $E_{0.12}$ defect level to titanium impurity. A defect level with energy $E_c - 0.18 \text{ eV}$ has also been reported and associated with a titanium impurity [11]. The $E_{0.12}$ and $E_{0.18}$ levels could both be a single defect occupying different geometrical positions in the material, where it is seen as $E_{0.12}$ when occupying a hexagonal site while it is seen as $E_{0.18}$ when occupying a cubic lattice site [14].

The $E_{0.69}$ level is a prominent defect that is found in 4H-SiC. While the defect level is widely agreed to be of intrinsic nature, there is no agreement on the exact structure of the defect. The possible structure of the defect has been attributed to a silicon vacancies, carbon vacancies, silicon and carbon antisite complexes [15-18]. The structure of the defect has essentially been linked to nearly all possible intrinsic defects that can be found in SiC. Low energy and high energy particle irradiation measurements have been performed to possibly link the defect structure of the defect to either carbon or silicon exclusively but this did not solve the puzzle [19, 20].

Figure 6 shows normalized DLTS spectra taken before irradiation, after irradiation and after annealing from 200 °C to 600 °C. After irradiation the $E_{0.69}$ level broadens and shows an increase in intensity. The broadening of the $E_{0.69}$ level after irradiation is possibly due to presence of more energy levels which may be contained within the level. The sample was then annealed to possibly separate these energy levels. After annealing at 200 °C, three defects $E_{0.42}$, $E_{0.62}$ and $E_{0.76}$ with energies $E_c - 0.42$ eV, $E_c - 0.62$ eV and $E_c - 0.76$ eV were observed. The apparent capture cross sections of the observed defects were calculated from Arrhenius plots to be 1×10^{-15} cm², 2×10^{-14} cm² and 1×10^{-14} cm² respectively.

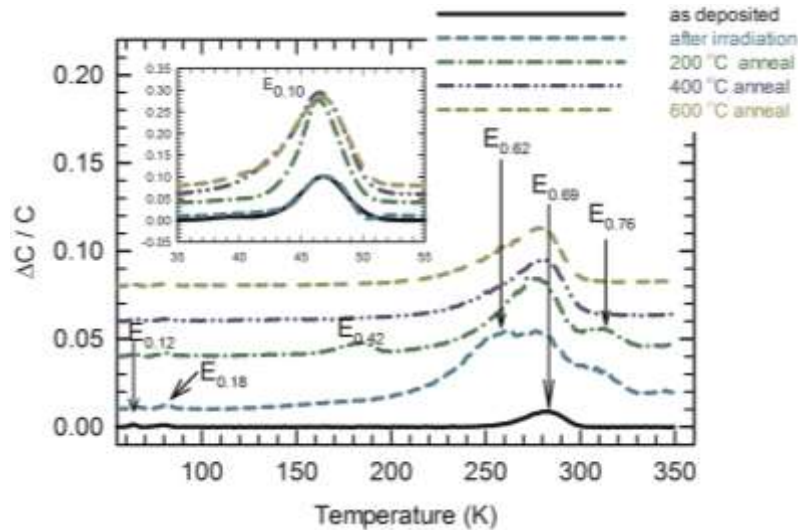


Figure 6 DLTS spectra for the as deposited sample, after alpha particle irradiation to fluence of 2.6×10^{10} cm⁻² and after successive annealing temperatures. Spectra obtained at constant reverse bias of -5V, filling pulse of -1 V and rate window of 2.5 s⁻¹

Defects $E_{0.42}$ and $E_{0.76}$ have been reported in previous studies [2, 11]. Level $E_{0.42}$ is attributed to silicon vacancies while $E_{0.76}$ has not been assigned any particular structure [21]. Doyle et al [2] observed the two defects after electron irradiation and isochronal annealing with the defects only being observed after annealing at 200 °C. Castaldini *et al.* [11], also observed the same defects after both electron and proton irradiation and suggests the defects are intrinsic. These levels were annealed out at 400 °C in this study. The fact that defects $E_{0.42}$ and $E_{0.76}$ were observed after the same particle fluence and annealed out after the same heat treatment suggests that the defects might be closely related structurally.

The concentration of the $E_{0.69}$ level increases significantly after irradiation and remains relatively stable up to the 600 °C annealing temperature. The possibility that this level is linked to carbon vacancies and / or interstitials or carbon divacancies can therefore be easily comprehended in the light of this increase in concentration after irradiation. Previous studies done on this defect suggest it could be a defect complex composed of several energy levels [18, 21]. Hemmingsson *et al.* [20] reported that the defect $E_{0.69}$, commonly referred to as the Z1/Z2 is composed of two closely spaced levels that have negative U behaviour. It was also established in this study that after alpha particle irradiation to a fluence of 2.6×10^{10} cm⁻², a defect with an energy of $E_c - 0.62$ eV appears on the lower temperature side of $E_{0.69}$. This defect is however not stable and was annealed out at 200 °C.

Depth concentrations of defects $E_{0.69}$ and $E_{0.76}$ were determined from Laplace-DLTS measurements by varying the voltages pulses and are presented in Figure 7. The depth concentration of defect $E_{0.69}$ was obtained before and after particle irradiation for comparison and an increase resulting from irradiation is clear. It is seen from the graph that the concentration of both defects is constant in the investigated depth range. This is in agreement with the prediction of SRIM simulations where the vacancy concentration is constant to a depth of ~ 24 μ m.

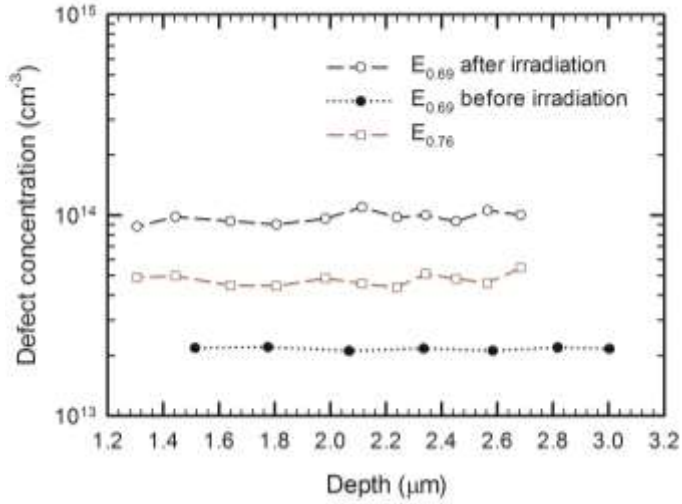


Figure 7 Depth concentration profiles for defects $E_{0.69}$ (before and after irradiation) and $E_{0.76}$

Levels $E_{0.12}$ and $E_{0.18}$ were not noticeably affected by irradiation. The concentration of the level $E_{0.10}$ increased after annealing at 200 °C without showing further changes at higher annealing temperatures. While the $E_{0.10}$ level is almost definitely a nitrogen impurity, it is not clear what the source of the increase in concentration after irradiation is. The defect parameters for the observed defects are summarised in Table 2.

Table 2 As grown and defects observed by DLTS in 4H-SiC after 5.4 MeV irradiation and annealing.

Trap level	$E_c - E_t$ (eV)	σ_n (cm ²)	N_T before irradiation (cm ⁻³)	N_T after irradiation (cm ⁻³)	Attribution
$E_{0.10}$	0.10	7×10^{-14}	9.4×10^{13}	6.0×10^{13}	N impurity - [22]
$E_{0.12}$	0.12	1×10^{-14}	2.2×10^{11}	2.3×10^{11}	Ti impurity- [21]
$E_{0.18}$	0.18	1×10^{-14}	5.4×10^{11}	6.0×10^{13}	Ti impurity- [11, 14]
$E_{0.42}$	0.42	1×10^{-15}	-	2.8×10^{13}	V_{Si} - [21]
$E_{0.69}$	0.69	2×10^{-14}	8.2×10^{12}	9.4×10^{13}	Z_1/Z_2 - [18]
$E_{0.62}$	0.62	-	-	-	-
$E_{0.76}$	0.76	1×10^{-14}	-	5.0×10^{13}	-

4. Conclusions

I - V , C - V and DLTS measurements were used to evaluate the effect of 5.4 MeV alpha-particle irradiation on nickel Schottky diodes fabricated on nitrogen doped 4H-SiC. After irradiation to fluence of 2.6×10^{10} cm⁻², the Schottky diodes retained rectification showing the radiation hardness of SiC. A large free carrier removal rate was obtained from C - V measurements indicating the presence of acceptor like defects as a result of irradiation. DLTS measurements revealed the presence of deep level defects before irradiation and three other deep level defects were observed after alpha-particle irradiation. The irradiation induced defects were all annealed out at temperatures below 600 °C.

5. Acknowledgements

The authors would like to acknowledge the National Research Foundation (NRF) of South Africa for financial support

References

- [1] K. Danno, D. Nakamura, T. Kimoto, Appl. Phys. Lett. **90** (2007) 202109.
- [2] J.P. Doyle, M.O. Aboelfotoh, B.G. Svensson, A. Schoner, N. Nordell, Diamond and Related Materials **6** (1997) 1388.
- [3] F. Roccaforte, C. Bongiorno, F. La Via, V. Raineri, Appl. Phys. Lett. **85** (2004) 6152.
- [4] A.A. Lebedev, A.I. Veinger, D.V. Davydov, V.V. Kozlovski, N.S. Savkina, A.M. Strel'chuk, J. Appl. Phys. **88** (2000) 6265.
- [5] K.P. Schoen, J.M. Woodall, J.A. Cooper, Jr., M.R. Melloch, Electron Devices, IEEE Trans. Electron. Devices **45** (1998) 1595.
- [6] S.K. Cheung, N.W. Cheung, Appl. Phys. Lett. **49** (1986) 85.
- [7] S. M. Sze, K.K. Ng, Physics of Semiconductor Devices, John Wiley & Sons, New Jersey, 2007.
- [8] F. Roccaforte, F. La Via, V. Raineri, R. Pierobon, E. Zanoni, J. Appl. Phys. **93** (2003) 9137.
- [9] F.D. Auret, S.A. Goodman, M. Hayes, M.J. Legodi, H.A. van Laarhoven, D.C. Look, Appl. Phys. Lett. **79** (2001) 3074.
- [10] T. Kimoto, A. Itoh, H. Matsunami, S. Sridhara, L. L. Clemen, R. P. Devaty, W.J. Choyke, T. Dalibor, C. Peppermuller, G. Pensl, Appl. Phys. Lett. **67** (1995) 2833.
- [11] A. Castaldini, A. Cavallini, L. Rigutti, F. Nava, S. Ferrero, F. Giorgis, J. Appl. Phys. **98** (2005) 053706.
- [12] A.O. Evwaraye, S.R. Smith, W.C. Mitchel, MRS Online Proceedings Library **410** (1995) 57.
- [13] C.Q. Chen, J. Zeman, F. Engelbrecht, C. Peppermüller, R. Helbig, Z.H. Chen, G. Martinez, J. Appl. Phys. **87** (2000) 3800.
- [14] N. Achtziger, W. Witthuhn, Appl. Phys. Lett. **71** (1997) 110.
- [15] T. Hiyoshi, T. Kimoto, Appl. Phys. Express **2** (2009) 091101.
- [16] L. Storasta, J.P. Bergman, E. Janzén, A. Henry, J. Lu, J. Appl. Phys. **96** (2004) 4909.
- [17] J. Zhang, L. Storasta, J. P. Bergman, N. T. Son, E. Janzén, J. Appl. Phys. **93** (2003) 4708.
- [18] I. Pintlilie, L. Pintlilie, K. Irmscher, B. Thomas, Appl. Phys. Lett. **81** (2002) 4841.
- [19] F.C. Beyer, C. Hemmingsson, H. Pedersen, A. Henry, J. Isoya, N. Morishita, T. Ohshima, E. Janzen, Phys. Scripta **T141** (2010) 014006.
- [20] C. Hemmingsson, N.T. Son, O. Kordina, J.P. Bergman, E. Janzen, J.L. Lindstrom, S. Savage, N. Nordell, J. Appl. Phys. **81** (1997) 6155.
- [21] T.A.G. Eberlein, R. Jones, P.R. Briddon, Phys. Rev. Lett. **90** (2003) 225502.
- [22] A. Castaldinia, A. Cavallinia, L. Polentaa, F.Navab, C. Canalic, C. Lanzierid, Appl. Surf. Sci. **187** (2002) 248.